Analysis and Design of Pavement Surface Mixtures for Traffic Noise Reduction

Center for Transportation, Environment, and Community Health

Final Report

by

Qing Lu, Manjriker Gunaratne, Mohammad Alharthai, Asad Elmagarhe

June 30, 2021

DISCLAIMER

TECHNICAL REPORT STANDARD TITLE PAGE

1. Report No.	2.Government Accession No.	3. Recipient's Catalog No.
4. Title and Subtitle Analysis and Design of Pavement Surface Mixtures for Traffic Noise Reduction		5. Report Date March 31, 2021 6. Performing Organization Code
7. Author(s) Qing Lu (ORCID ID 0000-0002-9120-9218), Manjriker Gunaratne, Mohammad Alharthai, Asad Elmagarhe		8. Performing Organization Report No.
9. Performing Organization Name and Address Department of Civil and Environmental Engineering University of South Florida Tampa, FL, 33620		10. Work Unit No. 11. Contract or Grant No. 69A3551747119
12. Sponsoring Agency Name and Address U.S. Department of Transportation 1200 New Jersey Avenue, SE Washington, DC 20590		13. Type of Report and Period Covered Final Report 10/01/2019 – 06/30/2021 14. Sponsoring Agency Code US-DOT

15. Supplementary Notes

16. Abstract

Road traffic noise pollutes the living environment and has adverse effects on public health. It may be reduced at its source by a quiet pavement surface. This study investigated the relationship between design parameters of porous asphalt mixtures placed at the pavement surface and the pavement acoustic performance. A mechanistic-empirical model was developed based on a microstructural model of the acoustic absorption of porous media and regression analysis of model parameters as functions of mixture design parameters, using a set of experimental data covering a range of porous asphalt mixture designs. This model may be used to predict the acoustic absorption of porous asphalt concrete, particularly at high frequencies (1000 Hz and above). Regression models were also developed to estimate the effect of mixture design, in terms of nominal maximum aggregate size, on tire-pavement noise at low frequencies. The impact of porous mixture design on pavement friction, in terms of skid resistance and hydroplaning speed, was also evaluated. A procedure was recommended to include the consideration of acoustic performance in the design of porous asphalt mixtures for road surfaces with frequent motor vehicle traffic.

17. Key Words	18. Distribution Statement
Porous Asphalt Mixture, Pavement Noise, Aggregate Gradation, Sound Absorption, Mixture Design	Public Access as well as a resulting journal manuscript submitted, based on which this report is developed.

19. Security Classif (of this report)	20. Security Classif. (of this page)	21. No of Pages	22. Price
Unclassified	Unclassified	31	

Form DOT F 1700.7 (8-69)

Abstract

Road traffic noise pollutes the living environment and has adverse effects on public health. It may be reduced at its source by a quiet pavement surface. This study investigated the relationship between design parameters of porous asphalt mixtures placed at the pavement surface and the pavement acoustic performance. A mechanistic-empirical model was developed based on a microstructural model of the acoustic absorption of porous media and regression analysis of model parameters as functions of mixture design parameters, using a set of experimental data covering a range of porous asphalt mixture designs. This model may be used to predict the acoustic absorption of porous asphalt concrete, particularly at high frequencies (1000 Hz and above). Regression models were also developed to estimate the effect of mixture design, in terms of nominal maximum aggregate size, on tire-pavement noise at low frequencies. The impact of porous mixture design on pavement friction, in terms of skid resistance and hydroplaning speed, was also evaluated. A procedure was recommended to include the consideration of acoustic performance in the design of porous asphalt mixtures for road surfaces with frequent motor vehicle traffic.

1 Introduction

Transportation is the major source of environmental noise, particularly in urban areas with high population density near or along transportation infrastructures such as road, railway, and airport (Berglund et al., 2000; Moudon, 2009). Noise is considered by the World Health Organization (WHO) as a harmful environmental pollutant and has adverse psychosocial and physiologic effects on public health (Berglund et al., 2000; Kim et al., 2012), ranging from auditory to non-auditory association (Basner et al., 2014). Noise pollution is a growing problem around the world. For example, a recent assessment of environmental noise within Europe revealed that more than 100 million people are exposed to long-term noise levels that are detrimental to their health (EEA, 2020).

The impacts of road traffic noise on health include sleep disturbances (Douglas and Murphy, 2016; Halonen et al., 2012), annoyance responses (Berglund and Lindvall, 1995), depression (Eze et al., 2020; Gille et al., 2016; Seidler et al., 2017), elevated risks for cardiovascular diseases (Seidler et al., 2016), potential mental health (Sygna et al., 2014), psychiatric disorder (Stansfeld et al., 1996), hearing loss, and cognitive performance inhibitions (Basner et al., 2014; Berglund and Lindvall, 1995). These impacts result from several major vehicle-related contributors to road traffic noise, including engine and exhaust noises, aerodynamic noise, and tire/pavement noise (Ramussen et al., 2007). The tire-pavement noise becomes dominant in the road traffic noise when vehicle speed exceeds certain values (i.e., 35 km/h for light vehicles and 50 km/h for heavy vehicles) (Keulen and Duškov, 2005). With the increasing use of electric vehicles, which do not produce engine or exhaust noise, the proportion of tire-pavement noise in the total traffic noise on roads is expected to be higher in the future. Reducing the tire-pavement noise, therefore, will play a more important role in health promotion for the public living along highways and streets.

Currently, the noise abatement measure allowed by the Federal Highway Administration (FHWA) for federally funded projects is noise barrier (FHWA, 2011). Recent research, however, has shown that the tire-pavement noise may be reduced by a noticeable level at its source by

adjusting the design of pavement surface (Ling et al., 2021; Lu et al., 2009b), thus reducing or even eliminating the need for expensive noise barriers that often have negative visual impact. Some existing pavement surface mixtures, such as open-graded friction course (OGFC) mixture that is designed to reduce vehicle hydroplaning potential during rain, may reduce the tire-pavement noise by 3 A-weighted decibels (dBA) compared to a conventional dense-graded asphalt concrete (DGAC) pavement surface (Lu et al., 2009b). This is because the high porosity (i.e., air-void content) of the OGFC mixture may absorb a noticeable amount of acoustical energy, particularly at high frequencies (Sakhaeifar et al., 2018). The recently updated FHWA Traffic Noise Model (TNM®), which is a software application required to be used on all Federal-aid highway projects for modeling traffic noise, has acknowledged such an effect and included open-graded asphalt pavement as one of the three pavement types in model inputs (Hastings, 2019; Rochat et al., 2012). Other variables, such as pavement surface macrotexture in terms of mean profile depth (MPD), nominal maximum aggregate size (NMAS, defined as one sieve size larger than the first sieve size to retain more than 10% of aggregates), and surface stiffness, have also been found to impact the tire-pavement noise (Sakhaeifar et al., 2018). Currently, however, there is no specification or widely accepted procedure for the design of pavement surface mixtures that include noise reduction as one of their target functions.

The main objective of this study is to analyze the relationship between mixture design variables and acoustic performance of the mixture and to develop a design procedure or guideline for pavement surface mixtures that considers noise reduction at the tire/pavement interface in addition to conventional functions (e.g., friction). Since asphalt pavement accounts for over 94 percent paved roads in the U.S. (NAPA, 2018) and porous (open-graded) asphalt mixture such as OGFC mixture is quieter than conventional dense-graded asphalt mixture (Lu et al., 2009b), this study focuses on porous asphalt mixture used in the pavement surface. This study intends to investigate what adjustments may be made to current designs of porous asphalt mixture for optimized pavement surface performance that includes noise reduction. The specific objectives are: (1) performing a literature review on the state-of-art of research on quiet pavements regarding major influential factors and mixture designs; (2) investigating the relationship between mixture design variables and mixture acoustic performance based on data collected from the literature and numerical analysis; (3) providing design recommendations for pavement surface mixtures for improved acoustic performance.

The remainder of the report is structured as follows. A review of the literature on pavement surface mixtures and their acoustic performance is summarized in Section 2. The methods for evaluating the acoustic performance of porous asphalt mixtures are described in Section 3. Section 4 analyzes the effects of mixture design parameters on tire/pavement noise and other pavement surface performance. Section 5 provides design recommendations of porous asphalt mixtures. Finally, the major findings are summarized in Section 6.

2 Literature review

The tire-pavement noise is affected by both tire and pavement. Tire design is optimized by tire companies for desired functions such as handling, friction, and noise, which are out of the scope of pavement engineering. For given tire features, pavement design can be adjusted to improve its acoustic performance without compromising other important functions related to safety, durability, and cost.

2.1 Mechanisms of tire-pavement noise generation

Sound is generated at the tire-pavement interface due to a number of mechanisms, occurring simultaneously and to varying degrees (Ramussen et al., 2007). The more prominent ones include tire tread impact, air pumping in between tire tread and pavement texture, stick-slip of tire rubber, and stick-snap of tire tread blocks, among which the air-pumping is the main source of tire-pavement noise (Ling et al., 2021). The tire-pavement noise is further amplified, often at certain frequencies, due to several mechanisms, including acoustical horn, Helmholtz resonance, pipe resonance, side wall vibrations, and cavity resonance (Ramussen et al., 2007). Generally, the horn effect is more significant than the other amplification mechanisms (Ling et al., 2021).

2.2 Pavement surface mixture designs and acoustic performance

The noise perceived by a person at the roadside includes sound waves traveling in different paths from the sound source (i.e., tire-pavement interface): directly in air, reflected from the pavement surface, and propagating through pavement surface media. Based on the noise generation mechanisms, pavement may lower the tire-pavement noise at its source by keeping a small and negative surface texture, a high surface porosity, and a low stiffness, in decreasing order of importance (Ramussen et al., 2007). Small and negative texture and low stiffness may reduce tire tread impact while high porosity may change air pumping and acoustical horn amplification. A porous pavement surface can also transform and attenuate sound energy when sound waves propagate through its interconnected pores. During sound wave propagation in a pore, viscous friction (viscosity effect) and thermoelastic damping (thermal effect) will dissipate some sound energy carried by the sound wave (Allard and Atalla, 2009). In this sense, noise may be further reduced along some of its propagation paths to the receiver at the roadside (Ling et al., 2021).

The desirable pavement surface features for quieter pavement can be achieved through surface mixture design. Compared to the conventional DGAC, some surface mixtures with low porosity have been found to be quieter due to their favorable surface texture features (Ling et al., 2021). Ultra-thin wearing course (UTWC) mixture and stone mastic asphalt (SMA) are two examples. The UTWC mixture combines gap gradation (most coarse aggregates in the size range of 4.75-9.5 mm) and emulsion asphalt and is placed at a thickness of 20-30 mm (Cui et al., 2020). The SMA is also a gap-graded asphalt mixture. The voids among its coarse aggregates are largely filled with mastic, which is a mix of asphalt binder, very fine aggregates, and stabilizer, so the air-void content of compacted SMA is comparable to that of DGAC, around 3-8% (Vázquez et al., 2019). Due to its well-structured coarse aggregate skeleton and rich mastic content, SMA has high resistance to both fatigue cracking and permanent deformation. The pavement surface texture of these mixtures, resulting mainly from the gap gradation, may mitigate the air-pumping effect and dissipate noise energy in the sound wave propagation path along pavement surface (Ling et al., 2021). SMA mixtures with smaller aggregate size are generally quieter due to a smoother surface (Vázquez et al., 2019). Thin overlay mixes (TOM's) used in Texas, which have a gap or dense gradation and a maximum aggregate size in the range of 4.75-9.5 mm, have also been found in field measurement to be quieter, even than permeable friction course (PFC) with larger maximum aggregate size (Smit et al., 2016). Due to their low porosity, however, the noise reduction performance of these mixtures is generally lower than porous mixtures of the same maximum aggregate size (Losa et al., 2013).

Prior work has shown that new pavements with open-graded asphalt surfaces generally emitted lower tire-pavement noise than new pavements with dense- or gap-graded asphalt surfaces (Lu et

al., 2009b), and the use of small aggregate size (e.g., a nominal maximum aggregate size [NMAS] of 4.75 mm) in porous asphalt mixture may result in low surface texture without much loss of porosity (Lu et al., 2009a; Lu and Harvey, 2011). A high porosity is the essential requirement for compacted porous asphalt mixture (named as porous asphalt concrete, PAC), used as either the pavement OGFC for improving wet traffic safety or the surface course of permeable pavements for managing stormwater runoff (Kayhanian et al., 2019), because porosity is highly correlated with permeability (Lu et al., 2009a). Compacted mixtures of the same air-void content, however, may have varying sound absorption performance due to differences in the size, shape, number, and distribution of pores in the mixtures (Losa and Leandri, 2012; Neithalath et al., 2005). For the same type of asphalt concrete with the same level of porosity, therefore, its composition design may be further explored to optimize its acoustic performance.

To minimize tire-pavement noise, a pavement stiffness that is close to the tire stiffness would be ideal (Ramussen et al., 2007). For given environmental and loading conditions, asphalt pavement surface stiffness is affected by asphalt binder type, aggregate gradation, and proportions of binder and aggregate. No matter how these mixture design variables change, however, the dynamic modulus of porous asphalt mixture is typically in the range of 500-10,000 MPa for common temperature and loading conditions (Nguyen et al., 2019), which is significantly higher than the modulus of tire rubber (around 1-10 MPa) (Baranowski et al., 2012; Hassan and Ahmed, 2018). This indicates that changing the binder type (e.g., polymer modified asphalt or asphalt rubber) or content will not significantly change the tire-pavement noise from the perspective of pavement stiffness reduction. Some field surveys revealed little correlation between tire-pavement noise and pavement surface stiffness (Sakhaeifar et al., 2018), but it was also observed that pavement surfaces with asphalt rubber mixtures were generally quieter than pavement surfaces with conventional asphalt binders in the long run (Freitas et al., 2019; Lu et al., 2009b). This is likely because porous mixtures with asphalt rubber are more durable in the field, leading to less pavement distresses that would increase tire-pavement noise. Some experimental pavements that use a poroelastic surface, which typically contains about 20% rubber (by weight) and polyurethane binder, can have a stiffness as low as 200 MPa (Jaskula et al., 2020) and significantly reduce the tire-pavement noise (Ejsmont et al., 2016). The low durability of such a surface, however, remains one key issue to be solved (Jaskula et al., 2020).

2.3 Acoustic absorption of porous asphalt concrete

In the design of porous asphalt mixtures, one key criterion is the air-void content of a compacted mixture. Air-void content is defined as the ratio of the volume of air in a compacted mixture specimen to the volume of the specimen, expressed in percentage. For porous asphalt concrete, it is typically required that the air-void content should be greater than 18% (Alvarez et al., 2006), and often less than 26%. This criterion does not consider the distribution and geometry of air voids, such as size, shape, and number, which may affect the acoustic performance of a pavement surface constructed with the mixture. Among the acoustic performance of a pavement surface, acoustic absorption is of particular importance since it reflects the capability of a pavement surface to reduce tire-pavement noise by absorbing and dissipating/transmitting sound energy. Acoustic absorption may be measured on a cylindrical specimen using an impedance tube in the laboratory. A prior study showed that the acoustic absorption measured on core samples from porous asphalt pavements had good positive correlation at high frequencies (1,000, 1,250, and 1,600 Hz) with the tire-pavement noise measured using the On-Board Sound Intensity

(OBSI) method (Ongel et al., 2007). At low frequencies (630 and 800 Hz), however, the correlation was weak (Ongel et al., 2007).

Acoustic absorption may also be estimated from theoretical acoustic models. The sound wave propagation through a porous medium whose pore structure is highly irregular, however, is a complex process and it is difficult to develop accurate theoretical models to predict the acoustic absorption of such porous media. Often empirical models, some of which are based on theoretical solutions to porous media with simple pore structures, are developed and applied, as discussed below.

Delany and Bazley developed phenomenological equations between characteristic acoustic impedance, air flow resistivity, and propagation constant in porous materials (Delany and Bazley, 1970). Their equations have been applied to designs of many sound absorbers. Due to their empirical nature, however, their equations can lead to unrealistic predictions and cannot be used to study the effect of pore morphology on sound absorption.

Based on the principle of electroacoustic analogy and acoustic impedance due to viscous effects, Lu et al. (Lu et al., 2000) developed a theory to predict the acoustic absorption coefficient of metallic foams with idealized semi-open cellular structures, and explored the correlation between acoustic absorption and pore parameters. This microstructural modeling approach was extended by Neithalath et al. to investigate the influence of pore structure on the acoustic absorption of enhanced porosity concrete (EPC) that has a porosity of 20-25% (Neithalath et al., 2005). Pores of variable cross sections were converted to a series of unit cells, each cell consisting of one cylindrical aperture and one cylindrical pore as illustrated in Figure 1 (which shows two unit cells), with the same porosity and same characteristic pore size (i.e., the median of pore sizes greater than 1 mm). A structure factor was used to account for the effect of lateral pores on acoustic absorption. The acoustic absorption coefficient for such a pore-aperture structure model was derived by representing the pores and apertures as series of resistors and inductors in parallel and the propagation of sound wave as the flow of electricity. Sound absorption due to thermal effects was ignored in this model due to their small impact in rigid framed porous materials (Neithalath et al., 2005). The microstructural model of EPC from Neithalath et al. was later extended to PAC by Losa and Leandri (Losa and Leandri, 2012). Four geometric parameters in the microstructural model (i.e., pore diameter D_P, pore length L_P, aperture diameter D_A, and aperture length L_A as shown in Figure 1) were determined for a range of PAC designs by fitting the model to the acoustic absorption spectra measured from PAC specimens by the impedance tube test. The determined pore geometric parameters were then related to four mixture parameters (i.e., air-void content, mineral dust content, number of compaction gyrations, and fractal dimension) using multiple regression analysis (Losa and Leandri, 2012). Their empirical models, however, are limited in application because the fractal dimension cannot be easily calculated and the number of gyrations is not available for PAC compacted in other ways such as by a roller, Marshall, or Hveem compactor.

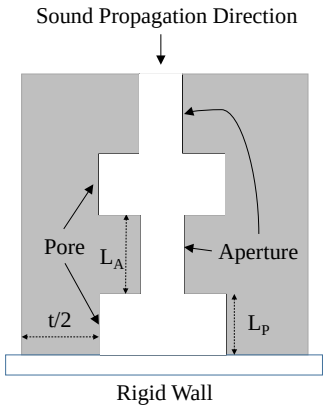

Figure 1. Pore-aperture model of porous medium for sound propagation (Neithalath et al., 2005)

Zwikker and Kosten developed theoretical formulas for sound propagation and impedance in cylindrical tubes and pores of a porous medium under normal incidence of sound (Zwikker and Kosten, 1949). In their model, sound propagation and dissipation in cylindrical pores of a porous medium layer are described at a macroscopic level as sound traveling in a layer of equivalent fluid with an effective density and bulk modulus (Allard and Atalla, 2009). These two parameters are frequency dependent and affected by the microstructure of the porous medium, such as diameter and length of pores. Different from Neithalath's model, the Zwikker and Kosten model considered both viscosity and thermal effects on acoustic absorption of the porous medium. To account for non-circular cross sections of straight pores and the tortuosity of realistic pores in porous media, shape factors were used to adjust sound propagation in pores (Allard and Atalla, 2009). The Zwikker and Kosten model was adopted by Wang et al. to model and optimize acoustic absorption of porous asphalt concrete (Wang et al., 2016). The pores with different sizes and shapes in a layer of porous asphalt concrete were first converted to cylindrical tubes that have an identical equivalent radius and an identical length, and are perpendicular to the layer surface. The equivalent radius was calculated based on equivalent total pore area measured from images of the PAC. The sound pressure and the acoustic particle velocity at the upper and bottom surfaces of the layer are related using a transfer matrix that is a function of the layer thickness and the effective density and bulk modulus of the porous material (Wang et al., 2016). The acoustic absorption coefficient in the frequency range of 100 to 1500 Hz for normal incidence was then predicted for various combinations of porosity (15-25%), equivalent pore radius (1-4 mm), and pore length (30-60 mm). Their parametric analysis results showed that porosity and pore length may play more significant roles in affecting acoustic absorption than pore radius, and increasing pore radius may reduce the maximum acoustic absorption coefficient when porosity is held constant. The pore parameters of the model, however, are neither directly equivalent to the geometric parameters of PAC nor directly related to mixture design parameters (e.g., aggregate gradation). Further work is needed to relate the model pore parameters to mixture design parameters so that the model may be used to guide porous asphalt mixture design.

3 Methods to estimate the acoustic performance of asphalt mixtures

As revealed in the literature review, a low-noise pavement surface should have desirable low surface texture and high surface porosity, which mainly affect the tire impact and vibration noise and the air pumping/resonance noise, respectively. The tire impact and vibration noise is more

significant at lower frequencies (< 1000 Hz) and the air pumping/resonance noise is more significant at higher frequencies (Sandberg and Ejsmont, 2002). In this study, the acoustic performance of asphalt mixtures is evaluated directly based on their acoustic absorption coefficient which mostly affects high-frequency tire-pavement noise and indirectly based on mixture design parameters affecting pavement surface texture which affect low-frequency noise.

3.1 Zwikker and Kosten microstructural model for acoustic absorption

The Zwikker and Kosten model applied by Wang et al. (2016) is implemented in this study to theoretically predict the acoustic absorption coefficient of a PAC layer. In this model, the PAC layer is treated as a porous medium with equally spaced cylindrical pores of identical radii (R) and identical lengths (d), as shown in Figure 2. The bottom of the PAC layer is supported by an impervious rigid wall and the surface of the PAC layer is in contact with the air. A plane incident sound wave travels perpendicularly to the PAC layer surface. The PAC layer is considered as a layer of equivalent fluid with an effective density, $\rho(\omega)$, and bulk modulus, $K(\omega)$. The absorption coefficient of the PAC for this normal incident sound wave, α, can be expressed as follows (Allard and Atalla, 2009).

$$\alpha = 1 - \left|\frac{p'(A')}{p(A')}\right|^2 = 1 - \left|\frac{Z(A')-Z_0}{Z(A')+Z_0}\right|^2 \quad (1)$$

where, $p'(A')$ is the pressure of the outgoing (reflected) sound wave at Point A' (at the surface of the PAC layer in the air); $p(A')$ is the pressure of the ingoing sound wave at Point A'; $Z(A')$ is the characteristic specific acoustic impedance at Point A'; Z_0 is the characteristic impedance of air (416.9 Pa·s/m at 15°C). By definition, characteristic specific acoustic impedance, Z, can be expressed as

$$Z = \frac{p}{u} = \sqrt{K(\omega)\cdot\rho(\omega)} \quad (2)$$

where, p is sound pressure; u is particle velocity; $K(\omega)$ is bulk modulus of the medium in which sound wave travels; $\rho(\omega)$ is effective density of the medium; ω is the angular frequency of the sound wave, $\omega = 2\pi f$, and f is the frequency of the sound wave.

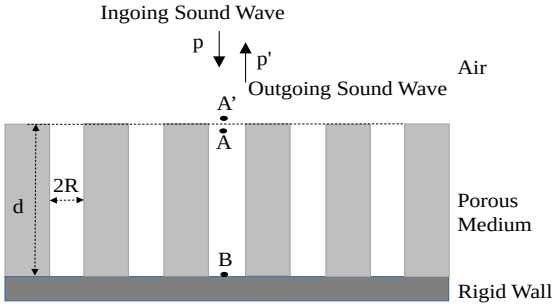

Figure 2. Zwikker and Kosten model of a PAC layer

At the interface of the air and the PAC, since the sound pressure and flow (i.e., volume velocity) are continuous, we have

$$p(A') = p(A) \tag{3}$$

$$u(A') = \phi u(A) \tag{4}$$

where, $p(A')$ and $u(A')$ are sound pressure and particle velocity at Point A', respectively; $p(A)$ and $u(A)$ are sound pressure and particle velocity at Point A, respectively; ϕ is porosity of PAC.

Within the porous medium (PAC) layer, the sound pressure and particle velocity at the surface ($p(A)$ and $u(A)$ at Point A) are related to the sound pressure and particle velocity at the bottom ($p(B)$ and $u(B)$ at Point B) using the transfer-matrix approach as follows (Wang et al., 2016):

$$\begin{bmatrix} p(A) \\ u(A) \end{bmatrix} = \begin{bmatrix} \cos(kd) & jZ_c \sin(kd) \\ jsin(kd)/Z_c & \cos(kd) \end{bmatrix} \begin{bmatrix} p(B) \\ u(B) \end{bmatrix} \tag{5}$$

where, k is angular wave number of the porous medium; d is the length of the pore; Z_c is the characteristic specific acoustic impedance of the porous medium; $j^2 = -1$. The angular wave number, k, can be expressed as

$$k = \omega\sqrt{\rho(\omega)/K(\omega)} \tag{6}$$

From Equations 3-5, it can be derived that

$$\begin{bmatrix} p(A') \\ u(A') \end{bmatrix} = \begin{bmatrix} \cos(kd) & jZ_c \sin(kd) \\ j\phi sin(kd)/Z_c & \phi\cos(kd) \end{bmatrix} \begin{bmatrix} p(B) \\ u(B) \end{bmatrix} \tag{7}$$

At the surface of the impervious rigid wall (Point B), it can be assumed that the particle velocity $u(B)$ is zero. Therefore, the characteristic specific acoustic impedance at Point A' is

$$Z(A') = \frac{p(A')}{u(A')} = \frac{\cos(kd)}{j\phi sin(kd)/Z_c} = -\frac{jZ_c \cot(kd)}{\phi} \tag{8}$$

The absorption coefficient in Equation 1 then becomes

$$\alpha = 1 - \left|\frac{-jZ_c \cot(kd) - \phi Z_0}{-jZ_c \cot(kd) + \phi Z_0}\right|^2 \tag{9}$$

Note that in Equation 9, the angular wave number, k, and the characteristic specific acoustic impedance, Z_c, of the porous medium are both functions of the bulk modulus, $K(\omega)$, and the effective density, $\rho(\omega)$, of the medium. Their expressions are given by the Zwikker and Kosten model as follows (Allard and Atalla, 2009):

$$\rho(\omega) = \rho_0 \left[1 + \frac{1}{\sqrt{3^2 + \frac{(aR)^2}{2}}} - j\frac{8}{(aR)^2}\sqrt{1 + \frac{(aR)^2}{32}}\right] \tag{10}$$

$$K(\omega) = \frac{\gamma P_0}{\gamma - (\gamma - 1)\left(1 - \frac{Nu}{j(aR)^2 Pr + Nu}\right)} \tag{11}$$

where, R is pore radius; ρ_0 is air density (1.213 kg/m^3); $a = \left(\frac{\omega\rho_0}{\eta}\right)^{0.5}$; η is shear viscosity of air (1.83×10^{-5} Pa·s or kg/(m·s)); P_0 is air pressure (1.013×10^5 Pa); γ is the ratio of specific heats (i.e., the ratio of the heat capacity at constant pressure to the heat capacity at constant volume) (1.4); Nu is Nusselt number (the ratio of convective to conductive heat transfer across a boundary) (3.10); Pr is Prandtl number (the ratio of momentum diffusivity to thermal diffusivity) (0.71).

As can be observed from Equations 2, 6, and 9-12, calculation of the absorption coefficient at various frequencies requires three model geometric parameters: pore radius (R), pore length (d), and porosity (ϕ) of the medium. The medium porosity (ϕ) is proportional to the square of pore radius (R) as follows:

$$\phi \propto nR^2 \tag{12}$$

where n is the number of pores in the porous medium.

3.2 Determination of model geometric parameters

The acoustic absorption coefficient of PAC specimens can be measured using the impedance tube test following the procedure in ASTM E 1050 (ASTM E 1050-19, 2019). The geometric parameters (R, d, ϕ) of the Zwikker and Kosten model for the PAC can then be estimated by minimizing the difference between the values measured by the impedance tube test ($\alpha_{measured}$) and the values predicted by the model ($\alpha_{predicted}$) for a number of PAC specimens. Specifically, the weighted residual sum of squares (WRSS), as defined by Equation 13, is minimized to find estimates of the geometric parameters.

$$WRSS = \sum_{f_i} w_{f_i}[\alpha_{measured}(f_i) - \alpha_{predicted}(f_i)]^2 \tag{13}$$

where the summation is over the nominal frequencies (f_i's) of one-third octave bands from 200 Hz to 1600 Hz (i.e., 200, 250, 315, 400, 500, 630, 800, 1000, 1250, and 1600 Hz); w_{f_i} is a weight value assigned at a frequency f_i. A higher weight value may be assigned to frequencies higher than 800 Hz due to higher correlation between the acoustic absorption measured in the laboratory and the OBSI measured in the field (Ongel et al., 2007). The nonlinear minimization problem can be solved using codes written in numerical computing languages such as MATLAB or the Solver Add-in program in Microsoft Excel.

3.3 Pavement surface texture

It has been shown that pavement surface texture with wavelengths in the range of 0.5 mm to 51 mm, known as macrotexture, has significant impact on tire-pavement noise (Ramussen et al., 2007). This range of texture is commonly characterized by the mean profile depth (MPD), as defined in ASTM E 1845 (ASTM E 1845-15, 2015). Field studies have shown that there is a strong correlation between MPD and tire-pavement noise (Hong et al., 2018; Lu et al., 2009b).

The relationship between tire-pavement noise and MPD will be explored based on field studies reported in the literature. Meanwhile, the relationship between MPD and porous mixture design parameters will be studied using regression analysis based on measurements from laboratory prepared specimens.

3.4 Experimental data

A set of impedance tube test results was obtained from cylindrical specimens of eight open gradations, as shown in Figure 3, prepared in a previous study (Lu et al., 2009a). As can be seen, the gradations covered a wide range of NMAS, from 4.75 mm to 19.0 mm, and variations in gradations of the same NMAS. Porous asphalt mixtures were prepared from these gradations using a quarried granite aggregate and both neat and modified asphalt binders.

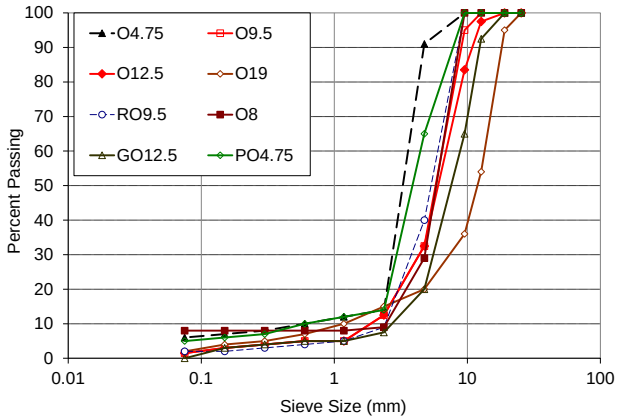

Figure 3. Aggregate gradations of porous asphalt mixtures

The list of porous asphalt mixtures included in the analysis is shown in Table 1. The PG 64-16 binder is neat asphalt while other binder types are asphalt modified with polymers or rubber. The optimum binder contents were determined primarily based on a draindown test that allows to retain as much as possible binder in the mixture without causing excessive binder loss due to draindown during construction (Caltrans, 2010; FDOT, 2014).

Table 1. Porous asphalt mixtures

Mixture Type	Binder Type	Binder Content (%)	NMAS (mm)
O4.75a	PG 64-16	7.9	4.75
O4.75b	Asphalt Rubber	9.5	4.75
O4.75c	PG 76-22TR	9.5	4.75
O4.75d	PG 58-34PM	7.9	4.75
O4.75e	PG 76-22PM	7.9	4.75
O4.75f	PG 64-16	7.9	4.75
PO4.75	Asphalt Rubber	8.4	6.00
O8	PG 64-16	6.4	8.00
O9.5a	PG 64-16	5.9	9.50
O9.5b	Asphalt Rubber	7.1	9.50
RO9.5	Asphalt Rubber	9.2	9.50
GO12.5	PG 76-22PM	6.3	12.50
O12.5	PG 64-16	5.9	12.50
O19	PG 64-16	5.0	19.00

The specimens used in the impedance tube test were cored from slabs compacted in the laboratory using a tandem steel wheel roller, which simulated the field compaction during asphalt pavement construction. The nominal slab thickness is 51 mm, but the actual thickness after compaction varied in the range of 30-76 mm for some specimens. Slab surfaces were

measured for their macrotexture in terms of MPD using a laser texture scanner. For each mixture type, at least two replicate specimens were cored from the slabs and measured for their acoustic absorption coefficient according to ASTM E 1050. During mixture preparation, the target air-void content of compacted slabs was 20%. The actual air-void contents of cored specimens ranged from 14% to 22%, as calculated from the theoretical maximum specific gravity measured in accordance with AASHTO T 209 (AASHTO T 209, 2014) and the bulk specific gravity measured using the paraffin method following AASHTO T 275 (AASHTO T 275, 2017).

4 Analysis of effects of mixture design parameters on surface performance

The effects of design parameters of porous asphalt mixtures on the acoustic performance of pavement surface are analyzed in this section along with other pavement surface performance such as friction.

4.1 Effects of mixture design parameters on acoustic absorption

To evaluate the effects of mixture design parameters on acoustic absorption of PAC, a two-step procedure was followed to estimate the relationship between design parameters and acoustic absorption:

(1) Following the method described in Section 3.2, the geometric parameters (R, d, ϕ) of the Zwikker and Kosten model were first estimated for specimens of mixtures listed in Table 1 based on their acoustic absorption values measured by the impedance tube test. A weight value of 2 was used in the WRSS formula. Other weight values greater than 1 were also tried and it was found that the estimation results were not changed significantly.
(2) The relationship between mixture design parameters and the geometric parameters estimated in the previous step was estimated using machine learning models.

In the first step, the nonlinear minimization problem was solved using the generalized reduced gradient (GRG) algorithm (Yeniay, 2005). Generally the Zwikker and Kosten model had a good fit to the test data. Figure 4 shows the comparison of the acoustic absorption spectra measured by the impedance tube test and those predicted by the Zwikker and Kosten model for two PAC specimens (GO12.5-2 and O8-1) after the model parameters were estimated through the nonlinear optimization. There were, however, a few specimens whose test data were not fitted well. These specimens were treated as outliers and excluded from further analysis.

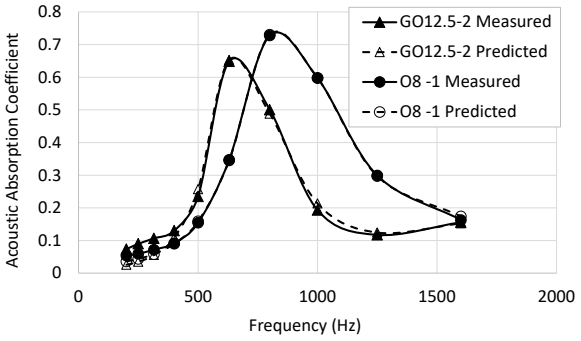

Figure 4. Comparison of measured and predicted acoustic absorption coefficients for two specimens

Finally, a total of 28 specimens were included in the analysis of the second step. Table 2 shows a summary of the specimens and corresponding estimated values of the three geometric parameters.

Table 2. Estimated values of geometric parameters of the Zwikker and Kosten model

Mix Type	Specimen ID	Air-void Content (%)	Specimen Thickness (m)	Porosity	Pore Radius (m)	Pore Length (m)
PO4.75	1	19.6	0.031	0.744	0.00066	0.087
O9.5b	1	19.1	0.051	0.507	0.00103	0.134
O9.5b	2	19.3	0.047	0.423	0.00091	0.130
RO9.5	1	18.1	0.049	0.478	0.00130	0.140
RO9.5	2	18.4	0.049	0.482	0.00106	0.139
O4.75d	1	16.4	0.050	0.662	0.00135	0.144
O4.75d	2	16.7	0.049	0.497	0.00178	0.176
O8	1	21.4	0.046	0.328	0.00061	0.097
O8	2	19.7	0.049	0.347	0.00075	0.111
O8	3	19.9	0.047	0.300	0.00086	0.134
O4.75f	1	18.5	0.048	0.486	0.00144	0.174
O12.5	1	19.7	0.076	0.309	0.00092	0.171
O12.5	2	20.3	0.072	0.383	0.00095	0.180
O19	1	16.0	0.070	0.628	0.00110	0.170
O19	2	15.4	0.076	0.788	0.00123	0.200
O19	3	14.8	0.067	0.324	0.00109	0.144
O19	4	14.1	0.049	0.554	0.00167	0.146
O19	5	15.2	0.047	0.412	0.00090	0.110
O4.75a	1	18.7	0.067	0.430	0.00156	0.176
O9.5a	1	20.8	0.047	0.346	0.00081	0.124
O9.5a	2	19.3	0.045	0.440	0.00092	0.130
GO12.5	1	19.4	0.047	0.404	0.00079	0.133
GO12.5	2	20.5	0.050	0.285	0.00086	0.123
GO12.5	3	19.2	0.050	0.282	0.00071	0.102
O4.75e	1	20.1	0.050	0.402	0.00110	0.135
O4.75e	2	20.2	0.049	0.497	0.00128	0.141
O4.75c	1	16.7	0.049	0.492	0.00117	0.139
O4.75c	2	17.1	0.048	0.468	0.00180	0.178

In the second step, machine learning models were applied to explore the relationship between the estimated geometric parameters and mixture design parameters. For porous asphalt mixtures, the following design parameters were considered: nominal maximum aggregate size (NMAS), percentage passing No. 4 sieve (4.75 mm) size (P4.75), percentage passing No. 8 sieve (2.36

mm) size (P2.36), percentage passing No. 200 sieve (0.075 mm) size (P0.075), fineness modulus, binder type, and binder content. The fineness modulus is an empirical value defined on the aggregate gradation. It is obtained by dividing the sum of percentages of aggregates retained on each of the series of sieves by 100. In general, a smaller fineness modulus indicates a finer gradation.

The machine learning models adopted in the study include regression trees and multiple linear regression (James et al., 2013). The tree-based regression segments the predictor space into a number of simple regions using a recursive binary splitting approach to minimize the residual sum of squares (RSS). The multiple linear regression assumes that the expected response variable is in the linear space of functions of the predictors. Compared to linear regression, tree-based regression does not have the linear relationship assumption and is easier to interpret (James et al., 2013). All the models were estimated in R, which is a free software environment for statistical computing and graphics (The R Foundation, 2021). In both modeling analyses, 80% of the data were randomly selected and used for model training and the rest 20% were used for model testing.

For the first geometric parameter, porosity (ϕ), seven design parameters (i.e., NMAS, P4.75, P2.36, P0.075, fineness modulus, binder type, and binder content) were selected as the potential predictors in modeling. Measured specimen air-void content was initially considered but later excluded from the predictor space due to the facts that (1) specimen air-void content was targeted towards 20% during compaction so it was not a design parameter, and (2) there was a poor correlation between specimen air-void content and porosity.

In the regression tree analysis for porosity, results showed that the tree construction generally used only two or three predictors and the type of predictors varied with the selection of the training data. One predictor, P2.36, however, persists in all trials of tree construction. Cross-validation shows that a tree of size 4 (i.e., four terminal nodes) leads to the minimum sum of squared errors for the test data, as shown in Figure 5(a). A tree of size 2, as shown in Figure 5(b), increases the sum of squared errors slightly but is simpler than the tree of size 4. Further tree analysis with bagging and random forest showed slight improvement in prediction accuracy. Since their models are difficult to interpret and present, however, they are not pursued further.

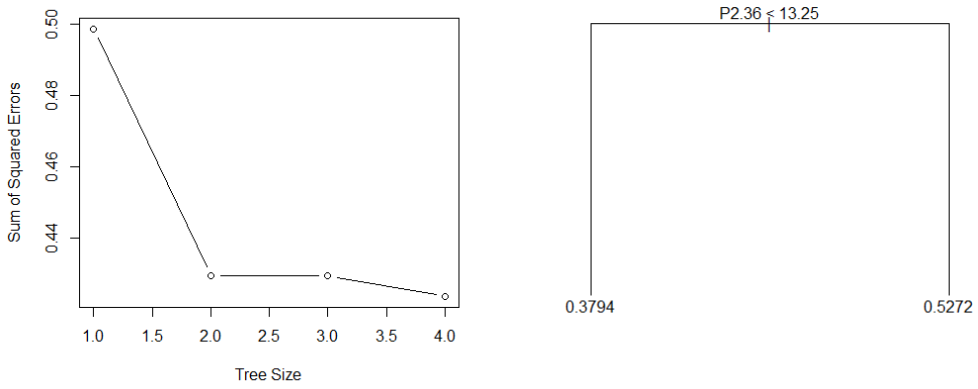

Figure 5. Regression tree for porosity: cross-validation error versus tree size (left); regression tree with two terminal nodes (right)

In the multiple linear regression, in order to find the best subset of predictors, a separate least squares regression was fit for each possible combination of the seven predictors and its prediction errors, in terms of adjusted R-squared (R^2), Mallow's C_p, and Bayesian information criterion (BIC), were computed. The best model was then selected based on these prediction errors. For porosity, the best subset selection showed 3, 2, and 2 predictors to be included in the best model based on maximum adjusted R^2, minimum C_p, and minimum BIC, respectively, as shown in Figure 6. Again, P2.36 exists in all these three sets of predictors, which is consistent with the regression tree results. Based on the maximum adjusted R^2, the three predictors included in the best subset are P2.36, binder content, and fineness modulus. The least squares estimations of the model coefficients are summarized in Table 3, with an adjusted R^2 of 0.34. Therefore, the estimated multiple linear regression model for porosity (ϕ) has the mathematical formula as

$$\phi = -0.945 + 0.035(P2.36) + 0.055(Binder\ Content) + 0.112(Fineness\ Modulus) \quad (14)$$

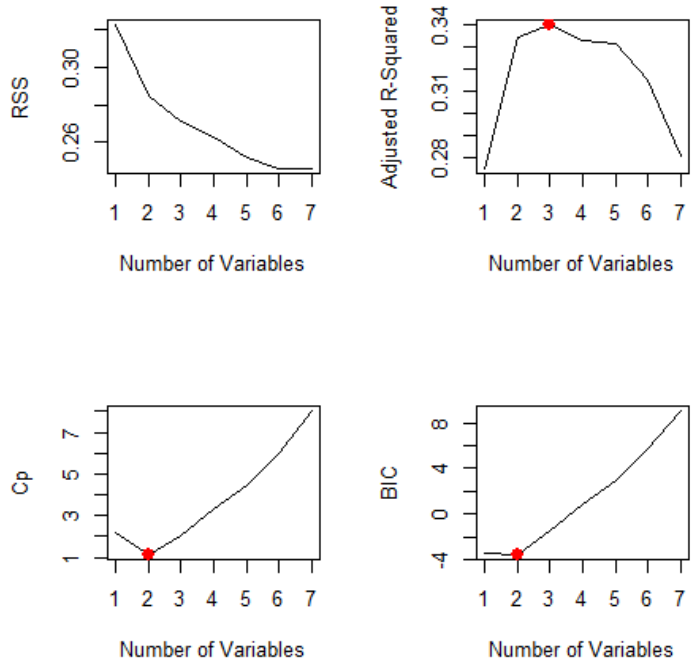

Figure 6. Measures of prediction errors for multiple regression models of porosity

Table 3. Estimated multiple linear regression model for porosity

Predictor	Estimate	Standard Error	t value	P-value
(Intercept)	-0.945	0.574	-1.647	0.113
P2.36 (%)	0.035	0.009	3.953	0.001
Binder Content (%)	0.055	0.026	2.119	0.045
Fineness Modulus	0.112	0.067	1.663	0.109

As can be seen from Table 3, the P-values associated with the predictors P2.36 and binder content are smaller than 0.05, indicating that at a significance level of 0.05, the null hypothesis that these two predictors do not affect porosity should be rejected. Among the three predictors in the model, P2.36 is most statistically significant. The signs of the coefficient estimates are all positive, indicating that more percentage passing the 2.36-mm sieve, higher binder content, or a finer gradation will lead to a higher porosity in the Zwikker and Kosten model. The low value of the adjusted R^2, however, suggests that a large share of variability in the porosity data is not explained by the multiple linear regression model.

Similar analyses were also performed for the other two model parameters. For pore radius (R), its regression tree construction generally used two predictors. Cross-validation showed that a tree of size 3 led to the minimum sum of squared errors for the test data. In multiple linear regression, the best subset selection showed 3, 2, and 2 predictors to be included in the best model for pore radius based on maximum adjusted R^2, minimum C_p, and minimum BIC, respectively. The predictor NMAS existed in all these three sets of predictors. Based on the maximum adjusted R^2, the three predictors included in the best subset are NMAS, binder content, and P4.75. The least squares estimations of the model coefficients are summarized in Table 4, with an adjusted R^2 of 0.56. The estimated multiple linear regression model for pore radius (R) is then

$$R = -5.657 \times 10^{-4} + (1.309 \times 10^{-5})(P4.75) + (5.869 \times 10^{-5})(Binder\ Content) + (6.35 \times 10^{-5})(NMAS) \quad (15)$$

Table 4. Estimated multiple linear regression model for pore radius (m)

Predictor	Estimate	Standard Error	t value	P-value
(Intercept)	-5.657e-4	4.791e-4	-1.181	0.249
P4.75 (%)	1.309e-5	2.494e-6	5.248	<0.001
Binder Content (%)	5.869e-5	5.192e-5	1.13	0.269
NMAS (mm)	6.350e-5	1.643e-5	3.865	0.001

The P-values in Table 4 show that P4.75 and NMAS are statistically significant in affecting pore radius at a significance level of 0.01. Among the three predictors in the model, P4.75 is most statistically significant. The signs of the coefficient estimates are all positive, indicating that more percentage passing the 4.75-mm sieve or a larger maximum aggregate size will lead to a higher pore radius in the Zwikker and Kosten model.

For pore length (d), specimen thickness was also included in the modeling as one potential predictor. The regression tree analysis showed that the tree construction generally used two or three predictors, in which specimen thickness persisted in most trials of tree construction. Cross-validation showed that a tree of size 3 led to the minimum sum of squared errors for the test data. In multiple linear regression, the best subset selection showed 3, 2, and 2 predictors to be included in the best model for pore length based on maximum adjusted R^2, minimum C_p, and minimum BIC, respectively. The predictor “specimen thickness” existed in all these three sets of predictors. Based on the maximum adjusted R^2, the three predictors included in the best subset are specimen thickness, P4.75, and P0.075. The least squares estimations of the model

coefficients are summarized in Table 5, with an adjusted R^2 value of 0.66. The estimated multiple linear regression model for pore length (d) is then

$$d = 0.02375 + (5.091 \times 10^{-4})(P4.75) - (2.237 \times 10^{-3})(P0.075) + 1.95(Thickness) \quad (16)$$

Table 5. Estimated multiple linear regression model for pore length (m)

Predictor	Estimate	Standard Error	t value	P-value
(Intercept)	2.375e-2	1.917e-2	1.239	0.227
P4.75 (%)	5.091e-4	1.285e-4	3.962	<0.001
P0.075 (%)	-2.237e-3	1.690e-3	-1.323	0.198
Thickness (m)	1.950	3.069e-1	6.355	<0.001

The P-values in Table 5 show that P4.75 and specimen thickness are statistically significant in affecting pore length at a significance level of 0.01. The signs of the coefficient estimates indicate that the specimen thickness is positively correlated with the pore length, which is expected. Increasing the aggregate percentage passing the 4.75-mm sieve would increase the pore length while increasing the aggregate percentage passing the 0.075-mm sieve may decrease the pore length. This suggests that increasing the proportion of fine aggregates (i.e., aggregates passing the 4.75-mm sieve) would increase the tortuosity of connected pores in porous asphalt concrete while increasing the proportion of mineral filler (i.e., aggregates passing the 0.075-mm sieve) may decrease the tortuosity of connected pores.

The statistical models presented in Equations 14-16 can be used with the Zwikker and Kosten model in Equation 9 to estimate the acoustic absorption coefficient of PAC based on the mixture design parameters of aggregate gradation and binder content. Mixture design optimization for maximum acoustic absorption then becomes possible in further quantitative analysis with other design considerations and requirements in a specific design scenario. A qualitative discussion of the effects of mixture design parameters on PAC acoustic absorption is presented below.

Prior parametric analysis of the Zwikker and Kosten model (Wang et al., 2016) revealed that: (a) increasing the porosity would reduce the peak acoustic absorption coefficient but increase the frequency range for the peak acoustic absorption; (b) increasing the pore radius would reduce the peak acoustic absorption coefficient but not change the frequency range for the peak acoustic absorption; (c) increasing the pore length would slightly increase the peak acoustic absorption but also reduce the frequency range for the peak acoustic absorption. For a quieter PAC pavement surface, higher acoustic absorption in the high frequency range (1000-2000 Hz) is desired since it is highly correlated with the tire-pavement noise measured by the OBSI method (Ongel et al., 2007). Based on this consideration, a smaller pore radius and a smaller pore length would be desired in the Zwikker and Kosten model to achieve higher acoustic absorption in the high frequency range. The desirable porosity level is less clear since it has opposite effects on peak acoustic absorption and frequency range. When the pore length is low, however, a lower porosity seems to be more desirable. From the previous discussions on the effects of mixture design parameters on the three model parameters, we may infer that a porous asphalt mixture

with the following features may result in lower air pumping/resonance noise at high frequencies (1000-2000 Hz):

- a smaller maximum aggregate size,
- a lower percentage passing the 4.75-mm sieve,
- a lower percentage passing the 2.36-mm sieve,
- a lower binder content, or
- a lower PAC layer thickness.

It needs to be noted that the empirical models (Equations 14-16) were developed based on data from PAC specimens of single layer and compacted by a roller compactor. For double-layer PAC or PAC compacted in other ways, the empirical models may have higher prediction errors.

4.2 Effects of mixture design parameters on pavement surface texture

There have been a few studies that explored the relationship between pavement macrotexture and tire/pavement noise. In a study conducted in South Korea (Hong et al., 2018), the tire-pavement noise (N_{CPX}), measured on DGAC and SMA pavements using the close-proximity method (CPX) in ISO Standard 11819-2 (ISO, 1997), was found to be correlated with MPD in a linear regression model: $N_{CPX}(dBA) = 3.13MPD(mm) + 95.57$ ($R^2 = 0.59$). In another study conducted in the U.S. (Liao et al., 2014), the tire-pavement noise measured using the OBSI method on OGFC pavements on a test track was positively correlated with MPD at frequencies of 1000 Hz and 1600 Hz but negatively correlated at 2500 Hz. In an earlier study completed by the principal investigator (PI), a number of in-service asphalt pavements in California were monitored over several years for their surface texture, using a laser profilometer, and tire-pavement noise using the OBSI method (Lu et al., 2009b). Multiple linear regression models were developed for the tire-pavement noise with MPD as one of the predictors. It was found that for open-graded pavement surfaces, 1 mm increase in MPD led to 2.16 dBA increase in the overall tire-pavement noise, 2.87 dBA increase in noise at 500 Hz, 4.04 dBA increase in noise at 1000 Hz, and 2.25 dBA decrease in noise at 4000 Hz (Lu et al., 2009b). It may be inferred from the studies above that an increase in pavement macrotexture generally increases the tire-pavement noise. For porous asphalt pavements, a higher MPD increases noise at lower frequencies (2000 Hz or less) but decreases noise at higher frequencies (over 2000 Hz).

The relationship between design parameters of porous asphalt mixtures and surface texture of PAC is explored in this study using the MPD data measured for the mixtures listed in Table 1. For each mixture, MPD was measured on multiple locations on the slab specimens of each mixture and the average value was reported. The mixture design information and average MPD values are summarized in Table 6.

For MPD, multiple linear regression analysis was performed using the mixture design parameters in Table 6 as potential predictors. A 5-fold cross-validation approach was taken to select the predictors that can minimize the test RSS (James et al., 2013). It was found that the test RSS was minimized when NMAS and binder content were included as predictors. The test RSS, however, only increased slightly when binder content was removed. When NMAS is included as the only predictor in the linear regression model, the adjusted R^2 is 0.76 and the estimated model is

$$MPD = 0.7237 + 0.0554(NMAS) \quad (17)$$

Table 6. Porous mixture design parameters and MPD

Mixture Type	P4.75	P2.36	P0.075	NMAS (mm)	Binder Content (%)	MPD (mm)
O4.75a	91.0	14.0	6.0	4.75	7.9	0.80
O4.75b	91.0	14.0	6.0	4.75	9.5	1.03
O4.75c	91.0	14.0	6.0	4.75	9.5	1.12
O4.75d	91.0	14.0	6.0	4.75	7.9	0.97
O4.75e	91.0	14.0	6.0	4.75	7.9	1.15
O4.75f	91.0	14.0	6.0	4.75	7.9	1.09
PO4.75	65.0	14.0	5.0	5.00	8.4	0.99
O8	29.0	9.0	8.0	8.00	6.4	1.17
O9.5a	32.5	12.5	1.5	9.50	5.9	1.06
O9.5b	32.5	12.5	1.5	9.50	7.1	1.26
RO9.5	40.0	9.0	2.0	9.50	9.2	1.32
GO12.5	20.0	7.5	3.0	12.50	6.3	1.33
O12.5	32.5	12.5	1.5	12.50	5.9	1.24
O19	20.0	15.0	2.0	19.00	5.0	1.95

The correlation between MPD and NMAS and the prediction performance of the estimated model are shown in Figure 7.

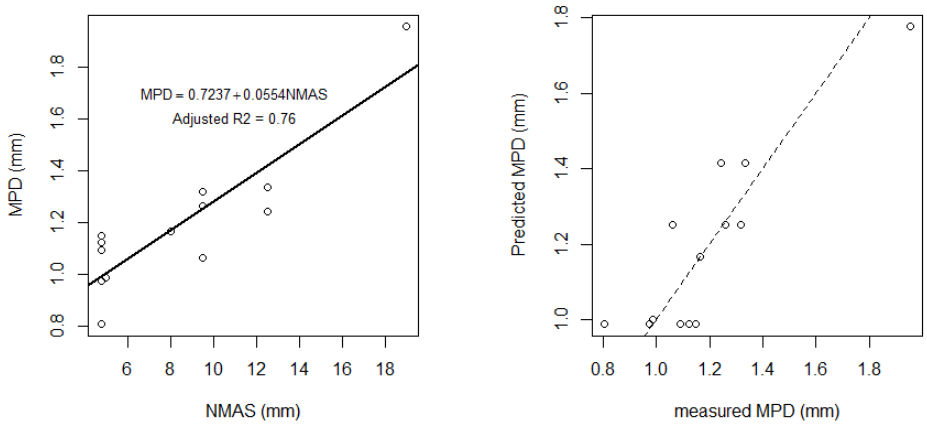

Figure 7. Correlation between MPD and NMAS of PAC

Combining Equation 17 and the findings from the prior field study (Lu et al., 2009b), the average increase in the tire-pavement noise, measured by the OBSI method, due to 1 mm increase in NMAS of PAC is about 0.0544 × 2.16 = 0.12 (dBA), 0.0544 × 2.87= 0.16 (dBA), and 0.0544 × 4.04 = 0.22 (dBA) for the overall noise, noise at 500 Hz, and noise at 1000 Hz, respectively.

4.3 Effects of mixture design parameters on pavement friction

When PAC is used for the pavement surface course, its main design function is to maintain sufficient pavement surface skid resistance and prevent hydroplaning during rain. It is known

that pavement skid resistance decreases with increasing vehicle speed at a rate affected by pavement macrotexture (Leu and Henry, 1978). In the well-known skid resistance model, known as the Penn State model as shown in Equations 18-20, both pavement surface microtexture and macrotexture play a role (Leu and Henry, 1978).

$$SN = SN_0 \exp[-\frac{PNG}{100} v] \quad (18)$$

$$SN_0 = -35 + 1.32BPN \quad (19)$$

$$PNG = 4.1MTD^{-0.47} \quad (20)$$

where, *SN* is skid number (a measure of skid resistance) at speed *v*; SN_0 is zero speed intercept related to microtexture; *PNG* is percent normalized gradient (hours/mile); *v* is vehicle speed (mph); *BPN* is British Pendulum number measured by a British Pendulum Tester (ASTM E 303-93, 2018), which is mainly a function of pavement microtexture; *MTD* is pavement mean texture depth (inches).

Pavement surface microtexture is mainly affected by the type of aggregate in the surface mixture. Commonly used aggregate types (e.g., granite, limestone, and basalt) can ensure sufficient microtexture. Pavement macrotexture in terms of MTD affects the rate at which skid resistance changes with vehicle speed. As can be seen from the Penn State model, a higher MTD corresponds to a lower reduction rate of skid resistance with the increase of vehicle speed.

Pavement surface macrotexture is governed by the gradation and size of aggregates (Flintsch et al., 2012). The discussion in Section 4.2 showed that the main mixture design parameter affecting PAC pavement macrotexture (in terms of MPD) was NMAS. It has also been revealed that there is a good correlation between MPD and MTD. For example, a recent study using 50 pavement segments of DGAC, SMA and OGFC surfaces developed a linear regression relationship between them, as shown in Equation 21 (Wang et al., 2011):

$$MTD = 0.247 + 0.785MPD \ \ (R^2 = 0.95) \quad (21)$$

A further study with more PAC pavements included found that MPD tended to increase with MTD nonlinearly for open-graded mixtures, as shown in Equation 22 (Praticò and Vaiana, 2015):

$$MPD = -0.109MTD^2 + 1.250MTD + 0.250 \ \ (R^2 = 0.93) \quad (22)$$

With Equations 17, 21 or 22, and the Penn State model, the effect of mixture design parameter (NMAS) on skid resistance may be quantitatively analyzed. However, since the macrotexture of PAC pavements, in terms of MPD or MTD, is generally over three times higher than that of DGAC pavements (Praticò and Vaiana, 2015), the skid resistance of PAC pavements generally will not be a concern in pavement surface mixture design.

Hydroplaning occurs when a thick water film on the pavement surface lifts the vehicle tire off the pavement surface, leading to a major loss of traction (Flintsch et al., 2012). The occurrence of hydroplaning is a function of vehicle speed. Several hydroplaning models have been developed to predict the hydroplaning speed (i.e., the vehicle speed at which hydroplaning

occurs). In a study completed by the authors, the hydroplaning speed is a function of water film thickness, wheel load, and tire pressure for light vehicles, as shown in Equation 23, and a function of water film thickness, tire pressure, and tire footprint aspect ratio for trucks, as shown in Equation 24 (Gunaratne et al., 2012).

$$v_p = WL^{0.2}p^{0.5}(\frac{0.82}{WFT^{0.06}} + 0.49) \quad (23)$$

$$v_p = 23.1p^{0.21}(\frac{1.4}{FAR})^{0.5}(\frac{0.268}{WFT^{0.651}} + 1) \quad (24)$$

where, v_p is hydroplaning speed (km/h); *WL* is wheel load (N); *p* is tire pressure (kPa); *WFT* is water film thickness (mm); *FAR* is tire footprint aspect ratio.

The water film thickness on PAC pavements can be estimated by Equation 25 (Anderson et al., 1998):

$$WFT = [\frac{nL(i-f)}{36.1S^{0.5}}]^{0.6} - MTD \quad (25)$$

where, *n* is Manning's roughness coefficient; *L* is drainage path length (inches); *i* is rainfall rate (inches/hour); *f* is permeability of pavement (inches/hour); *S* is slope of drainage path (mm/mm); *MTD* is mean texture depth (inches).

The Manning's n reflects the hydraulic roughness of a surface and is a function of the surface texture nature. For PAC pavements, it may be estimated from a regression model (Anderson et al., 1998):

$$n = \frac{1.490S^{0.306}}{N_R^{0.424}} \quad (26)$$

where, N_R is Reynold's number, $N_R = \frac{q}{\mu}$; q is quantity of flow per unit width ($m^3/s/m$); μ is kinematic viscosity of water. It is noted that Equation 26 was developed using data from PAC pavements with MTD in the range of 1.25-2.13 mm. For the porous asphalt mixtures in Table 6, the MTD estimated from MPD using Equation 21 is generally below 1.25 mm when the NMAS is smaller than 12.5 mm. Therefore, higher prediction errors may occur when Equation 26 is applied to PAC with small NMAS.

From Equations 23-26, it can be observed that the mixture parameters that affect the hydroplaning speed are mainly permeability and MTD. A high permeability and a high MTD lead to a low water film thickness and therefore a high hydroplaning speed. From Equation 17 and 21 or 22, we know that a higher NMAS leads to a higher MTD. The permeability of asphalt concrete is highly positively correlated with its air-void content (Lu et al., 2009b; Mogawer et al., 2002). Therefore, for a higher hydroplaning speed, a higher air-void content is desirable in the PAC.

5 Design recommendations of porous asphalt mixtures

The discussion in this section applies to porous asphalt mixtures used in pavements that experience frequent motor vehicle traffic, in which they are often referred to as OGFC mixtures

in the US. The porous asphalt mixtures for permeable pavements and the gap- and dense-graded mixtures reviewed in Section 2.2 (i.e., UTWC mixtures, SMA, and TOM) are out of the scope of this study.

Currently, among the transportation agencies that place the OGFC mixtures on their roads, the mixture design procedures are diverse but many generally involve the following steps: selecting trial aggregate gradations within the allowable ranges, selecting binder type and potential additives (e.g., fiber, hydrated lime, and liquid antistripping agents), and determining an optimum binder content. Design manuals or standard specifications are available to specify the allowable gradation ranges, binder type, additive types and dosages for various traffic and environmental conditions. In many US states, the optimum binder content is mainly determined based on different variants of a draindown test (AASHTO T 305, 2014; Caltrans, 2010; FDOT, 2014). Volumetric criteria and/or performance test requirements have been adopted by some agencies to refine the gradation, binder content, and additives for better mixture performance. For example, in the OGFC mixture design developed by the National Center for Asphalt Technology (NCAT) and implemented in the American Society for Testing Materials (ASTM) standards (ASTM D 7064-08, 2013), it requires that the voids in coarse aggregate of compacted mixture (VCA_{mix}) be equal to or less than the dry-rodded voids in coarse aggregate of the coarse aggregate fraction (VCA_{DRC}) to ensure stone-on-stone contact in the mixture. Abrasion loss on aged and unaged specimens from a Cantabro test, air-void content, and moisture sensitivity from a modified Lottman test (AASHTO T 283, 2014) need to be evaluated in finalizing the design. The Georgia Department of Transportation (GDOT) determines its OGFC mixture binder content not only from the draindown test, but also from a procedure that determines the surface capacity of coarse aggregate, and from a modified Marshall design method (Varadhan, 2004). It also evaluates the mixture moisture sensitivity by a boil test. Good summaries of various porous asphalt mixture design methods used in the US and in other countries may be found in the literature (Alvarez et al., 2006; Kayhanian and Harvey, 2020).

The design of porous asphalt mixtures for reduced traffic noise may follow the current design procedures for OGFC mixtures with an additional measure on the mixture acoustic performance. To this end, the following procedure is recommended:

1. Select a current OGFC mixture design method.
2. Within the allowable ranges of aggregate gradation, select trial gradations towards
    - a smaller nominal maximum aggregate size,
    - a lower percentage passing the 4.75-mm sieve,
    - a lower percentage passing the 2.36-mm sieve.
3. Follow the selected design method to determine the optimum binder content; Within the allowable range, select towards a lower binder content.
4. Use the mechanistic-empirical model developed in this study (Equations 9 and 14-16) to predict the acoustic absorption coefficient (at frequencies of 1000 Hz and above) of the trial mixtures determined in the previous steps.
5. In combination with the average increases in the tire-pavement noise (at frequencies of 1000 Hz and lower) per unit increase of NMAS as estimated in Section 4.2, compare the trial mixtures for their high-frequency acoustic absorption coefficients and relative changes in the low-frequency tire-pavement noise, and select the mixture with a higher high-frequency acoustic absorption coefficient and a lower low-frequency tire-pavement noise.

6. Subject the mixture to further volumetric and performance evaluation, if there are any, specified in the selected OGFC mixture design method.
7. Depending on the particular design scenarios (e.g., high rainfall intensity, multiple lanes, or low pavement surface drainage gradient), the mixture permeability and MTD may need to be measured (or estimated from air-void content and NMAS, respectively) to estimate the hydroplaning speed using the models discussed in Section 4.3.

As can be seen, the recommended adjustments to the current OGFC mixture design are mainly on the aggregate gradation. This is feasible because there is a range of variability in the gradation ranges specified by different agencies and the gradation ranges are pretty wide, as shown in Table 7 for some typical examples (ASTM E 1845-15, 2015; Caltrans, 2018; FDOT, 2021; Kayhanian and Harvey, 2020). This table shows that the allowable ranges for percentages passing the 4.75-mm and 2.36-mm sieves and the NMAS, which have significant effects on the geometric parameters of the Zwikker and Kosten model, are wide among different agencies.

Table 7. Typical OGFC gradation design ranges (percent passing by mass)

Sieve	ASTM	FDOT	TxDOT (PG 76)	TxDOT (A-R)	Caltrans (½ inch)	Caltrans (1 inch)	MDOT	NDOT
25.4 mm	-	-	-	-	-	99-100	-	-
19.0 mm	100	100	100	100	-	85-96	-	-
12.5 mm	85-100	85-100	80-100	95-100	95-100	55-71	100	100
9.5 mm	35-60	55-75	35-60	50-80	78-89	-	80-100	90-100
4.75 mm	10-25	15-25	1-20	0-8	28-37	10-25	15-30	35-55
2.36 mm	5-10	5-10	1-10	0-4	7-18	6-16	10-20	-
1.18 mm	-	-	-	-	-	-	-	5-18
0.60 mm	-	-	-	-	0-10	-	-	-
0.075 mm	2-4	2-5	1-4	0-4	0-3	0-6	2-4	0-4

By incorporating a new dimension of design objective, the feasible solution space is reduced due to additional constraints imposed by the additional objective. Compromises need to be made to balance multiple design objectives. For example, this study recommends a smaller NMAS and a lower binder content to favor lower tire-pavement noise at low frequencies and higher acoustic absorption at high frequencies. These changes, however, would lead to a lower hydroplaning speed and a lower resistance to permanent deformation. Decisions on how to balance conflicting design objectives will depend on the relative importance of the objectives in a specific design scenario.

6 Conclusions

As an environmental pollutant, road traffic noise has adverse impact on public health. Proper design of pavement surface can help alleviate the road traffic noise generated at the tire-pavement interface. This study investigated the relationship between mixture designs and acoustic performance of porous asphalt pavement surfaces and recommended a procedure to consider noise reduction in the pavement surface mixture design. The following conclusions are obtained from the study:

1. A microstructural model with simple pore geometry can be used to characterize the acoustic absorption performance of porous asphalt concrete (PAC).
2. With empirical models that correlate PAC mixture design parameters and the microstructural model parameters, the acoustic absorption performance of PAC can be estimated from the mixture design parameters.
3. The low-frequency tire-pavement noise is affected by the macrotexture of pavement surface, which can be estimated from the nominal maximum aggregate size (NMAS) of PAC.
4. For porous asphalt mixtures, within the ranges of aggregate gradation allowed by current design methods for open-graded friction course (OGFC) mixtures, it is recommended to select a gradation towards a smaller NMAS, a lower percentage passing the 4.75-mm sieve, or a lower percentage passing the 2.36-mm sieve.

It needs to be noted that the empirical models that correlate mixture designs to pavement acoustic performance were developed based on a small sample size of mixture specimens. The estimated model parameters, therefore, would have high variance. This may be improved, however, if data from more mixture design variants and specimens become available in further studies in the future.

References

AASHTO T 209, 2014. Standard method of test for theoretical maximum specific gravity (Gmm) and density of asphalt mixtures. American Association of State Highway and Transportation Officials (AASHTO), Washington, D.C.

AASHTO T 275, 2017. Standard method of test for bulk specific gravity (Gmb) of compacted asphalt mixtures using paraffin-coated specimens. American Association of State Highway and Transportation Officials (AASHTO), Washington, D.C.

AASHTO T 283, 2014. AASHTO T 283: Standard method of test for resistance of compacted asphalt mixtures to moisture-induced damage. American Association of State Highway and Transportation Officials (AASHTO), Washington, D.C.

AASHTO T 305, 2014. AASHTO T 305: Standard method of test for determination of draindown characteristics in uncompacted asphalt mixtures. American Association of State Highway and Transportation Officials (AASHTO), Washington, D.C.

Allard, J.F., Atalla, N., 2009. Propagation of Sound in Porous Media: Modelling of Sound Absorbing Materials, 2nd ed, John Wiley and Sons, Ltd. Elsevier Ltd.

Alvarez, A.E., Martin, A.E., Estakhri, C.K., Button, J.W., Glover, C.J., Jung, S.H., 2006. Synthesis of current practice on the design, construction, and maintenance of porous friction courses (No. FHWA/TX-06/0-5262-1). College Station.

Anderson, D.A., Huebner, R.S., Reed, J.R., Warner, J.C., Henry, J.J., 1998. Improved surface drainage of pavements (No. NCHRP Web Document 16). Washington, DC.

ASTM D 7064-08, 2013. Standard practice for open-graded friction course (OGFC) mix design, ASTM International. West Conshohocken, PA. https://doi.org/10.1520/D7064

ASTM E 1050-19, 2019. Standard test method for impedance and absorption of acoustical materials using a tube, two microphones and a digital frequency analysis system, ASTM International. West Conshohocken, PA.

ASTM E 1845-15, 2015. Standard practice for calculating pavement macrotexture mean profile depth, ASTM International. West Conshohocken, PA.

ASTM E 303-93, 2018. Standard test method for measuring surface frictional properties using the british pendulum tester, ASTM International. West Conshohocken, PA.

Baranowski, P., Bogusz, P., Gotowicki, P., Małachowski, J., 2012. Assessment of mechanical properties of offroad vehicle tire: Coupons testing and FE model development. Acta Mech. Autom. 6, 17–22.

Basner, M., Babisch, W., Davis, A., Brink, M., Clark, C., Janssen, S., Stansfeld, S., 2014. Auditory and non-auditory effects of noise on health. Lancet (London, England) 383, 1325–1332. https://doi.org/10.1016/S0140-6736(13)61613-X

Berglund, B., Lindvall, T., 1995. Community noise, Center for Sensory Research, Stockholm.

Berglund, B., Lindvall, T., Schwela, D.H., 2000. New WHO guidelines for community noise. Noise Vib. Worldw. 31, 24–29. https://doi.org/10.1260/0957456001497535

Caltrans, 2018. Standard specifications, California Department of Transportation. California Department of Transportation, Sacramento, CA. https://doi.org/10.1201/9781482296761-14

Caltrans, 2010. Method of test for optimum bitumen content (OBC) for open graded friction course (No. California Test 368). Sacramento, California.

Cui, W., Wu, K., Cai, X., Tang, H., Huang, W., 2020. Optimizing gradation design for ultra-thin wearing course asphalt. Materials (Basel). 13. https://doi.org/10.3390/ma13010189

Delany, M.E., Bazley, E.N., 1970. Acoustical properties of fibrous absorbent materials. Appl. Acoust. 3, 105–116. https://doi.org/10.1016/0003-682X(70)90031-9

Douglas, O., Murphy, E., 2016. Source-based subjective responses to sleep disturbance from transportation noise. Environ. Int. 92–93, 450–456. https://doi.org/10.1016/j.envint.2016.04.030

EEA, 2020. Environmental noise in Europe - 2020, Publications Office of the European Union. Luxembourg. https://doi.org/10.2800/686249

Ejsmont, J.A., Goubert, L., Ronowski, G., Świeczko-Zurek, B., 2016. Ultra low noise poroelastic road surfaces. Coatings 6. https://doi.org/10.3390/coatings6020018

Eze, I.C., Foraster, M., Schaffner, E., Vienneau, D., Pieren, R., Imboden, M., Wunderli, J.M., Cajochen, C., Brink, M., Röösli, M., Probst-Hensch, N., 2020. Incidence of depression in relation to transportation noise exposure and noise annoyance in the SAPALDIA study. Environ. Int. 144. https://doi.org/10.1016/j.envint.2020.106014

FDOT, 2021. Standard specifications for road and bridge construction. Florida Department of Transportation, Tallahassee, FL.

FDOT, 2014. Florida method of test for determining the optimum asphalt binder content of an open-graded friction course using the pie plate method (No. FM 5-588). Gainesville, Florida.

FHWA, 2011. Highway traffic noise : analysis and abatement guidance. Washington, DC.

Flintsch, G.W., McGhee, K.K., Izeppi, E.D.L., Najafi, S., 2012. The Little Book of Tire Pavement Friction (No. Version 1). Blacksburg, VA.

Freitas, E., Silva, L., Vuye, C., 2019. The influence of pavement degradation on population exposure to road traffic noise. Coatings 9. https://doi.org/10.3390/coatings9050298

Gille, L.A., Marquis-Favre, C., Morel, J., 2016. Testing of the European Union exposure-response relationships and annoyance equivalents model for annoyance due to transportation noises: The need of revised exposure-response relationships and annoyance equivalents model. Environ. Int. 94, 83–94. https://doi.org/10.1016/j.envint.2016.04.027

Gunaratne, M., Lu, Q., Yang, J., Metz, J., Jayasooriya, W., Yassin, M., Amarsiri, S., 2012. Hydroplaning on Multi Lane Facilities (No. BDK 84 977-14). Tampa, FL.

Halonen, J.I., Vahtera, J., Stansfeld, S., Yli-Tuomi, T., Salo, P., Pentti, J., Kivimäki, M., Lanki, T., 2012. Associations between nighttime traffic noise and sleep: The Finnish public sector study. Environ. Health Perspect. 120, 1391–1396. https://doi.org/10.1289/ehp.1205026

Hassan, F., Ahmed, S., 2018. Dynamic response of machine foundation resting on sand-granulated tyre rubber mixtures. MATEC Web Conf. 162, 1021. https://doi.org/10.1051/matecconf/201816201021

Hastings, A.L.., 2019. Technical manual: Traffic Noise Model 3.0, Report #: FHWA-HEP-20-

012. Washington, DC.

Hong, S.J., Park, S.W., Lee, S.W., 2018. Tire-pavement noise prediction using asphalt pavement texture. KSCE J. Civ. Eng. 22, 3358–3362. https://doi.org/10.1007/s12205-018-9501-3

ISO, 1997. Acoustics — Measurement of the influence of road surfaces on traffic noise — Part 2: The close-proximity method (No. ISO 11819-2). International Organization for Standardization.

James, G., Witten, D., Hastie, T., Tibshirani, R., 2013. An introduction to statistical learning with application in R, 1st ed. Springer.

Jaskula, P., Szydlowski, C., Stienss, M., Rys, D., Jaczewski, M., Pszczola, M., 2020. Durable poroelastic wearing course SEPOR with highly modified bitumen, in: Transportation Research Procedia. Elsevier B.V., pp. 882–889. https://doi.org/10.1016/j.trpro.2020.02.080

Kayhanian, M., Harvey, J.T., 2020. Optimizing rubberized open-graded friction course (RHMA-O) mix designs for water quality benefits: Phase I: literature review (No. UCPRC-RR-2019-03). Davis, CA.

Kayhanian, M., Li, H., Harvey, J.T., Liang, X., 2019. Application of permeable pavements in highways for stormwater runoff management and pollution prevention: California research experiences. Int. J. Transp. Sci. Technol. 8, 358–372. https://doi.org/10.1016/j.ijtst.2019.01.001

Keulen, W. Van, Duškov, M., 2005. Inventory study of basic knowledge on tyre/road noise. Road Hydraul. Eng. Div. Rijkswaterstaat 106.

Kim, M., Chang, S.I., Seong, J.C., Holt, J.B., Park, T.H., Ko, J.H., Croft, J.B., 2012. Road traffic noise: annoyance, sleep disturbance, and public health implications. Am. J. Prev. Med. 43, 353–360. https://doi.org/10.1016/j.amepre.2012.06.014

Leu, M.C., Henry, J.J., 1978. Prediction of skid resistance as a function of speed from pavement texture measurements. Transp. Res. Rec. 1, 7–13.

Liao, G., Sakhaeifar, M.S., Heitzman, M., West, R., Waller, B., Wang, S., Ding, Y., 2014. The effects of pavement surface characteristics on tire/pavement noise. Appl. Acoust. 76, 14–23. https://doi.org/10.1016/j.apacoust.2013.07.012

Ling, S., Yu, F., Sun, D., Sun, G., Xu, L., 2021. A comprehensive review of tire-pavement noise: Generation mechanism, measurement methods, and quiet asphalt pavement. J. Clean. Prod. 287, 125056. https://doi.org/10.1016/j.jclepro.2020.125056

Losa, M., Leandri, P., 2012. A comprehensive model to predict acoustic absorption factor of porous mixes. Mater. Struct. Constr. 45, 923–940. https://doi.org/10.1617/s11527-011-9808-8

Losa, M., Leandri, P., Licitra, G., 2013. Mixture design optimization of low-noise pavements. Transp. Res. Rec. 25–33. https://doi.org/10.3141/2372-04

Lu, Q., Fu, P., Harvey, J.T., 2009a. Laboratory evaluation of the noise and durability properties of asphalt surface mixes (No. UCPRC-RR-2009-07), University of California Pavement Research Center.

Lu, Q., Harvey, J., 2011. Laboratory evaluation of open-graded asphalt mixes with small

aggregates and various binders and additives. Transp. Res. Rec. 61–69. https://doi.org/10.3141/2209-08

Lu, Q., Kohler, E., Harvey, J.T., Ongel, A., 2009b. Investigation of noise and durability performance trends for asphaltic pavement surface types: three-year results (No. UCPRC-RR-2009-01).

Lu, T.J., Chen, F., He, D., 2000. Sound absorption of cellular metals with semiopen cells. J. Acoust. Soc. Am. 108, 1697–1709. https://doi.org/10.1121/1.1286812

Mogawer, W.S., Mallick, R.B., Teto, M.R., Crockford, W.C., 2002. Evaluation of permeability of Superpave mixes (No. NETCR 34). North Dartmouth, MA.

Moudon, A.V., 2009. Real noise from the urban environment. How ambient community noise affects health and what can be done about it. Am. J. Prev. Med. 37, 167–171. https://doi.org/10.1016/j.amepre.2009.03.019

NAPA, 2018. Fast facts [WWW Document]. 2018-2019. URL https://www.asphaltpavement.org/uploads/documents/GovAffairs/NAPA Fast Facts 11-02-14 Final.pdf (accessed 11.2.20).

Neithalath, N., Marolf, A., Weiss, J., Olek, J., 2005. Modeling the influence of pore structure on the acoustic absorption of enhanced porosity concrete. J. Adv. Concr. Technol. 3, 29–40. https://doi.org/10.3151/jact.3.29

Nguyen, T.H., Ahn, J., Lee, J., Kim, J.-H., 2019. Dynamic modulus of porous asphalt and the effect of moisture conditioning. Mater. (Basel, Switzerland) 12, 1230. https://doi.org/10.3390/ma12081230

Ongel, A., Kohler, E., Nelson, J., 2007. Acoustical absorption of open-graded, gap-graded and dense-graded asphalt pavements (No. UCPRC-RR-2007-12). Davis and Berkeley.

Praticò, F.G., Vaiana, R., 2015. A study on the relationship between mean texture depth and mean profile depth of asphalt pavements. Constr. Build. Mater. 101, 72–79. https://doi.org/10.1016/j.conbuildmat.2015.10.021

Ramussen, R.O., Bernhard, R.J., Sandberg, U., Mun, E.P., 2007. The little book of quieter pavements (No. FHWA-IF-08-004), Federal Highway Administration. Washington, DC.

Rochat, J.L., Hastings, A.L., Read, D.R., Lau, M., 2012. FHWA traffic noise model (TNM) pavement effects implementation study: Progress report 1, Report #: FHWA-HEP-12-034.

Sakhaeifar, M., Banihashemrad, A., Liao, G., Waller, B., 2018. Tyre–pavement interaction noise levels related to pavement surface characteristics. Road Mater. Pavement Des. 19, 1044–1056. https://doi.org/10.1080/14680629.2017.1287770

Sandberg, U., Ejsmont, J.A., 2002. Tyre/road noise: reference book. Informex, Sweden.

Seidler, A., Hegewald, J., Seidler, A.L., Schubert, M., Wagner, M., Dröge, P., Haufe, E., Schmitt, J., Swart, E., Zeeb, H., 2017. Association between aircraft, road and railway traffic noise and depression in a large case-control study based on secondary data. Environ. Res. 152, 263–271. https://doi.org/10.1016/j.envres.2016.10.017

Seidler, A., Wagner, M., Schubert, M., Dröge, P., Römer, K., Pons-Kühnemann, J., Swart, E., Zeeb, H., Hegewald, J., 2016. Aircraft, road and railway traffic noise as risk factors for

heart failure and hypertensive heart disease—A case-control study based on secondary data. Int. J. Hyg. Environ. Health 219, 749–758. https://doi.org/10.1016/j.ijheh.2016.09.012

Smit, A., Trevino, M., Garcia, N.Z., Buddhavarapu, P., Prozzi, J., 2016. Selection and design of quiet pavement surfaces (No. FHWA/TX-16/0-6819-1). Austin.

Stansfeld, S., Gallacher, J., Babisch, W., Shipley, M., 1996. Road traffic noise and psychiatric disorder: Prospective findings from the Caerphilly study. Br. Med. J. 313, 266–267. https://doi.org/10.1136/bmj.313.7052.266

Sygna, K., Aasvang, G.M., Aamodt, G., Oftedal, B., Krog, N.H., 2014. Road traffic noise, sleep and mental health. Environ. Res. 131, 17–24. https://doi.org/10.1016/j.envres.2014.02.010

The R Foundation, 2021. The R project for statistical computing [WWW Document]. URL https://www.r-project.org/ (accessed 1.12.21).

Varadhan, A., 2004. Evaluation of open-graded and bonded friction course for Florida. Univ. Florida. University of Florida.

Vázquez, V.F., Terán, F., Luong, J., Paje, S.E., 2019. Functional performance of stone mastic asphalt pavements in Spain: Acoustic assessment. Coatings 9, 1–15. https://doi.org/10.3390/COATINGS9020123

Wang, H., Ding, Y., Liao, G., Ai, C., 2016. Modeling and optimization of acoustic absorption for porous asphalt concrete. J. Eng. Mech. 142, 04016002. https://doi.org/10.1061/(asce)em.1943-7889.0001037

Wang, W., Yan, X., Huang, H., Chu, X., Abdel-Aty, M., 2011. Design and verification of a laser based device for pavement macrotexture measurement. Transp. Res. Part C Emerg. Technol. 19, 682–694. https://doi.org/10.1016/j.trc.2010.12.001

Yeniay, O., 2005. A comparative study on optimization methods for the constrained nonlinear programming problems. Math. Probl. Eng. 2, 165–173. https://doi.org/10.1155/MPE.2005.165

Zwikker, C., Kosten, C.W., 1949. Sound absorbing materials. Elsevier Pub. Co., New York.